2023 International Conference on Sampling Theory and Applications (SampTA) | 979-8-3503-2885-1/23/$31.00 ©2023 IEEE | DOI: 10.1109/SampTA59647.2023.10301401

Largest Angle Path Distance for Multi-Manifold Clustering

Haoyu Chen
Department of Mathematics
University of Utah
Salt Lake City, Utah 84112
Email: haoyu.chen@utah.edu

Anna Little
Department of Mathematics
Utah Center for Data Science
University of Utah
Salt Lake City, Utah 84112
Email: little@math.utah.edu

Akil Narayan
Department of Mathematics
Scientific Computing & Imaging Inst.
University of Utah
Salt Lake City, Utah 84112
Email: akil@sci.utah.edu

Abstract—**We propose a novel, angle-based path metric for the multi-manifold clustering problem. This metric, which we call the *largest-angle path distance (LAPD)*, is computed as a bottleneck path distance in a graph constructed on d-simplices of data points. When data is sampled from a collection of d-dimensional manifolds which may intersect, the method can cluster the manifolds with high accuracy and automatically detect how many manifolds are present. By leveraging fast approximation schemes for bottleneck distance, this method exhibits quasi-linear computational complexity in the number of data points. In addition to being highly scalable, the method outperforms existing algorithms in numerous numerical experiments on intersecting manifolds, and exhibits robustness with respect to noise and curvature in the data.**

I. Introduction

The analysis of high-dimensional data poses significant challenges; for example the dimension frequently exceeds the sample size, making traditional statistical frameworks untenable, and standard algorithms become computationally intractable. However in many applications, real data concentrates around low-dimensional structures, and leveraging this low dimensional structure is critical for overcoming the curse of dimensionality. In the simplest case, data concentrates on a single low-dimensional subspace or manifold. A more flexible, realistic model considers data lying on a collection of low-dimensional structures. Modeling each low-dimensional structure separately allows for a data representation which is sparse and efficient, and the first step in such a process is to partition the data into the underlying low dimensional structures. In this article we thus consider the *multi-manifold clustering* (MMC) problem, in which data points $X = \{x_i\}_{i=1}^n$ are drawn from a collection of manifolds $\mathcal{M}_1 \cup \ldots \cup \mathcal{M}_k$, and one seeks to recover the manifold labels $\ell_i \in [k]$ up to permutation.

Multi-manifold clustering is a generalization of (linear) subspace clustering, which is useful in many applications such as imaging [10, 4] and video segmentation [17]. The most popular and successful subspace clustering methods utilize spectral clustering with an affinity matrix which leverages self-expressive representations, for example SSC [8] and LLR [14]; other methods include [20, 5, 19, 11, 16, 6, 23, 25]. However, frequently the assumption that data lies on a collection of linear subspaces is too strong, and thus algorithms have been developed to handle nonlinear data structures, often modeled as multiple manifolds. Such a multi-manifold modeling assumption can be useful for motion segmentation and unsupervised image classification [15, 22, 24], for dynamic pattern identification and optical flow [9, 21], and for classification of text on webpages and in news stories [26]. The recent survey [1] taxonomizes MMC methods into three categories: (1) locality preserving, (2) kernel based, and (3) neural network based. Locality preserving methods leverage the local geometric structure of the manifolds; kernel based methods attempt to map the data into a high-dimensional space where linear subspace methods can be applied; neural network approaches seek to *learn* a useful embedding for MMC.

Our approach is a locality preserving method which leverages local angle information to define an appropriate distance/affinity. However our method avoids explicit approximation of local tangent planes as in [2], as well as explicit curvature or angle constraints as in [3, 18]. Instead we first estimate the intrinsic dimension d of the manifolds using an existing algorithm, and then propose the following novel pipeline:

1) (Simplex graph) Given nodes X, construct a weighted graph $\mathcal{G}_S$ on d-simplices formed from local nodes in X, where weights are assigned as angles between d-simplices.
2) (LAPD on simplices) Define distances between d-simplices as the bottleneck shortest path distance in $\mathcal{G}_S$.
3) (nLAPD on landmarks) Choose landmark nodes from X and use simplex LAPD to define a node-level nLAPD between landmarks.
4) (SC on landmarks) Construct a graph Laplacian on the landmarks using LAPD, and apply spectral clustering to partition the landmarks.
5) (Lift to all nodes) Extend the classification to all nodes via a LAPD nearest neighbor classifier.

Two primary advantages of the above approach are (i) it can reliably learn the number of manifolds, which is an assumed input parameter to most MMC algorithms, and (ii) it can be implemented in computational complexity that is quasi-linear with respect to the size of X, while most other methods are at least quadratic. The rest of the paper is organized as follows. Section II discusses the construction of LAPD on the simplices, i.e. steps (1) and (2); Section III then discusses how to use LAPD for MMC, i.e. steps (3)-(5); Section IV reports on numerical experiments investigating the performance of the proposed method; Section V discusses future research directions.

II. Construction of LAPD

We assume we have data points $X = \{x_1, \ldots, x_n\}$ sampled from a collection of k manifolds $\mathcal{M}_1 \cup \ldots \cup \mathcal{M}_k$, possibly polluted with noise. We first estimate the intrinsic dimension d of the data using the MSVD algorithm [13], requiring only quasi-linear cost. With this dimension d in hand, we must next identify local collections of points that can form simplices. We accomplish this with an unweighted annulus kNN graph on X. Fixing integers K_1, K_2 with $K_1 < K_2$, we let $\mathcal{G}_X$ be the graph which connects x_i, x_j if x_i is the I^{th} nearest neighbor of x_j or x_j is the I^{th} nearest neighbor of x_i, for any I satisfying $K_1 \leq I \leq K_2$; $K = K_2 - K_1$ denotes the kNN *bandwidth* which we assume is $O(1)$. The value of K_1 is chosen large enough so that simplices are formed on scales above the level of noise in X, and K_2 is chosen small enough so that simplices are formed on scales low enough to emulate the intrinsic curvature of the manifolds. Such Annulus graphs were also essential in [18]. The connections in $\mathcal{G}_X$ are then used to construct local d-simplices, specifically we define the set of valid simplices as:

$$S = \{\Delta \subseteq X : |\Delta| = d + 1, (x, y) \in E_X \;\; \forall x, y \in \Delta\}, \tag{1}$$

where E_X are the edges in $\mathcal{G}_X$. If $d = 2$, then simplices are triangles; and if $d = 3$, simplices are tetrahedra. We now form a weighted graph $\mathcal{G}_S = (S, E_S, W_S)$ on the simplices as follows: we connect Δ_i, Δ_j if $|\Delta_i \cap \Delta_j| = d$, i.e. they share a common face. The angle $\theta(\Delta_i, \Delta_j)$ between connected simplices is computed as the angle formed by vectors normal to the common face and passing through the non-common vertices. More specifically, letting x_i, x_j denote the points in Δ_i, Δ_j which are not in $\Delta_i \cap \Delta_j$ and picking some center $x_0 \in \Delta_i \cap \Delta_j$, we define

$$\begin{aligned} v_i &= (x_i - x_0) - P_{\Delta_i \cap \Delta_j}(x_i - x_0) \\ v_j &= (x_j - x_0) - P_{\Delta_i \cap \Delta_j}(x_j - x_0) \\ \theta(\Delta_i, \Delta_j) &= \arccos\left(\frac{\langle v_i, v_j \rangle}{\|v_i\| \cdot \|v_j\|}\right), \end{aligned}$$

where $P_{\Delta_i \cap \Delta_j}$ denotes projection onto the span of $\{x_s - x_0 : x_s \in \Delta_i \cap \Delta_j\}$, which is $d - 1$ dimensional. We weight the resulting edge $(\Delta_i, \Delta_j) \in E_S$ by $W_S(\Delta_i, \Delta_j) = \max\{\pi - \theta(\Delta_i, \Delta_j), \delta\}$, where $\theta(\Delta_i, \Delta_j)$ is the angle between the simplices and $\delta = 10^{-8}$ is a tolerance parameter selected to ensure that adjacent simplices are connected with non-zero weights. When two simplices form a "flat" connection, $\theta \approx \pi$ and $W_S(\Delta_i, \Delta_j) \approx 0$; but if the simplices "bend", $W_S(\Delta_i, \Delta_j)$ becomes large.

We now define the LAPD between any two simplices $S_1, S_2 \in S$ as follows.

Definition II.1 (LAPD). *Let $\mathcal{P} = \mathcal{P}(S_1, S_2)$ be the set of all simplex paths connecting S_1, S_2 in $\mathcal{G}_S$, i.e. any $\{\Delta_1, \ldots, \Delta_L\} \in \mathcal{P}$ satisfies $\Delta_1 = S_1, \Delta_L = S_2$, and $W_S(\Delta_s, \Delta_{s+1}) > 0$ for $1 \leq s \leq L - 1$. Then*

$$LAPD(S_1, S_2) := \min_{\{\Delta_1, \ldots, \Delta_L\} \in \mathcal{P}} \; \max_{1 \leq s \leq L-1} W_S(\Delta_s, \Delta_{s+1}). \tag{2}$$

Algorithm 1: Simplex LAPD

```
Input: $X = \{x_1, \dots, x_n\}$, intrinsic dim. $d$, NN
       range $K_1, K_2$, tolerance $\delta$
Output: LAPD on simplex set $S$
% Form annulus kNN graph $\mathcal{G}_X$
$\mathcal{G}_X \leftarrow (X, E_X)$, where $(x_i, x_j) \in E_X$ if $x_i, x_j$
  are $I^{\text{th}}$ NN's for $K_1 \leq I \leq K_2$
% Create set of valid simplices $S$
$S \leftarrow$ define by (1)
% Create angle-based weighted simplex graph $\mathcal{G}_S$
$\mathcal{G}_S \leftarrow (S, E_S, W_S)$, where $(\Delta, \Box) \in E_S$ if share
  face and $W_S(\Delta, \Box) = \max\{\pi - \theta(\Delta, \Box), \delta\}$
% Compute bottleneck distances in $\mathcal{G}_S$
$\text{LAPD}(\Delta, \Box) \leftarrow$ compute according to (2)
```

The entire LAPD construction is summarized in Algorithm 1. The computational cost is as follows: (1) annulus *kNN* construction is $O(K_2 D C^d n \log n)$ using cover trees; (2) constructing adjacency on simplices is $O(DK^{d+1}n)$; (3) running LLPD on $\mathcal{G}_S$ is $O(K^d n \log n)$ assuming $d, K = O(1)$.

III. LAPD for multi-manifold clustering

We now utilize the previously constructed simplex LAPD to obtain a landmark-based, node-level classification into manifold components. We first identify simplices that are "far enough" away from a manifold intersection so that they have a clear classification. We accomplish this by noting that such a simplex Δ will also have close-by neighbors on the same manifold, and so the LAPD between Δ and its close neighbors will be small. Thus, for a fixed K_3, we compute the maximum LAPD between Δ and its K_3 closest neighbors:

$$K_3\text{NN}(\Delta) = \min_{N \subseteq S, |N| = K_3} \max_{\Box \in N} \text{LAPD}(\Delta, \Box)\,.$$

Then we call simplices whose $K_3\text{NN}(\Delta)$ is small enough, say smaller than $\tau > 0$, as "denoised":

$$S_D = \{\Delta \in S : K_3\text{NN}(\Delta) \leq \tau\}\,.$$

From these denoised simplices, we select landmarks and proceed to assign node classifications. We randomly choose $m < n$ landmark nodes from $X_D = \cup_{\Delta \in S_D} \cup_{x \in \Delta} \{x\}$; for notational convenience, we will denote the landmarks as $x_1, \dots, x_m$ and the non-landmarks as $x_{m+1}, \dots, x_n$. The node-level nLAPD between all landmarks is then defined as follows:

$$\text{nLAPD}(x_i, x_j) = \min_{\Delta, \Box \in S \,:\, x_i \in \Delta, x_j \in \Box} \text{LAPD}(\Delta, \Box)\,.$$

Note since each node can be contained in multiple simplices, the nLAPD between two nodes is the minimum LAPD between any pair of simplices containing them. Let D_{LM} denote the resulting $m \times m$ nLAPD distance matrix with entries $\text{nLAPD}(x_i, x_j)$.

In the case that the number of manifolds k is given, we simply perform hierarchical clustering (HC) on D_{LM} to partition the landmarks; we refer to this method as k-LAPD in Section IV. We used average linkage HC in our experiments, but results were robust with respect to choice of linkage function. However, a significant advantage of our approach is highlighted when k is unknown: in this case we apply spectral clustering on (the graph Laplacian corresponding to) D_{LM} to *simultaneously* learn k and cluster the landmarks. Theoretical guarantees for a similar procedure using the Euclidean distance-based LLPD metric on nodes is given in [12], and our future work will extend these results to LAPD.

We now extend the partition on the landmarks via nearest neighbor classifier. For $i \in [m]$, let $\ell(i) \in [k]$ denote the landmark manifold labels for x_i. Then for each $j > m$, we compute $\ell(j)$ by finding the smallest nLAPD distance to x_j from the landmarks:

$$\ell(j) = \ell(\arg\min_{i \leq m} \text{nLAPD}(x_j, x_i))\,.$$

Spectral clustering on the landmarks is a fast $O(m^2)$ operation, and the classification extension costs $O(mnK^{2d})$. Thus the total cost of LAPD is $O\left((K_2 D C^d + K^d) n \log n + (DK^{d+1} + mK^{2d})n\right)$, i.e. quasi-linear dependence on the sample size n and linear dependence on the ambient dimension D.

IV. Numerical experiments

In this section, we investigate the performance of our proposed algorithm, by comparing it to competing state-of-the-art methods: LocPCA [2], PBC [3], and SMCE [7]. LocPCA uses spectral clustering with affinities which depend on discrepancies between local tangent planes; PBC employs

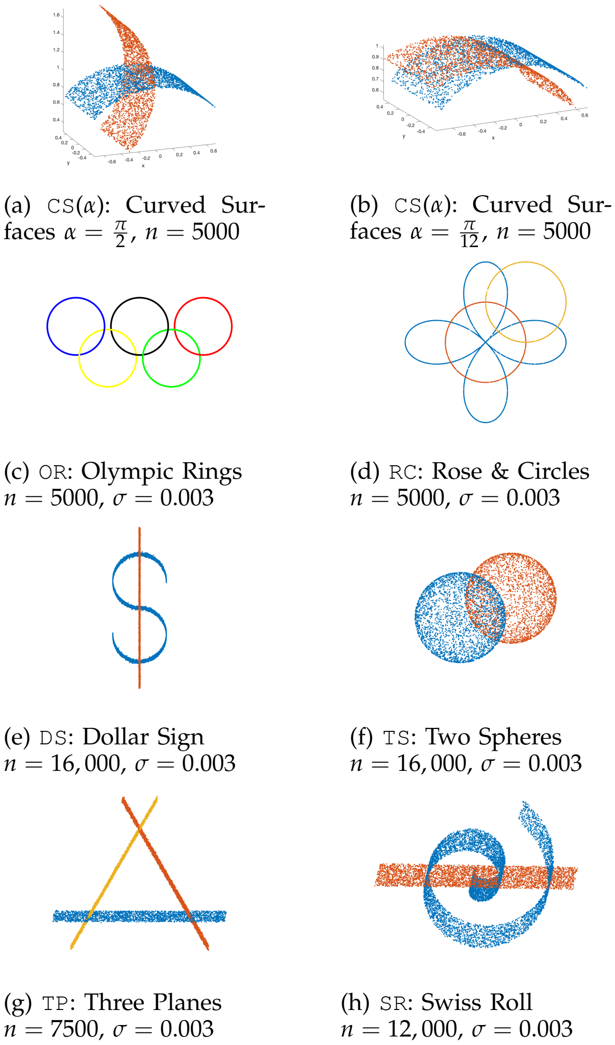
(a) $\texttt{CS}(\alpha)$: Curved Surfaces $\alpha = \frac{\pi}{2}$, $n = 5000$

(b) $\texttt{CS}(\alpha)$: Curved Surfaces $\alpha = \frac{\pi}{12}$, $n = 5000$

(c) $\texttt{OR}$: Olympic Rings $n = 5000$, $\sigma = 0.003$

(d) $\texttt{RC}$: Rose & Circles $n = 5000$, $\sigma = 0.003$

(e) $\texttt{DS}$: Dollar Sign $n = 16,000$, $\sigma = 0.003$

(f) $\texttt{TS}$: Two Spheres $n = 16,000$, $\sigma = 0.003$

(g) $\texttt{TP}$: Three Planes $n = 7500$, $\sigma = 0.003$

(h) $\texttt{SR}$: Swiss Roll $n = 12,000$, $\sigma = 0.003$

Figure 1: Synthetic data sets of size n, embedded in ambient space $\mathbb{R}^{10}$, polluted by ambient isotropic Gaussian noise with covariance $\sigma^2\mathbf{I}$. For Curved Surfaces ($\texttt{CS}$) we perform experiments both with noiseless data $\sigma = 0$ and noisy data $\sigma = 0.003$.

curvature-constrained shortest paths; SMCE utilizes sparsity and locality to estimates tangent plane structure. In particular, LocPCA is the only method among these with theoretical guarantees. All these competing methods require the number of clusters k as an input, but LAPD learns k automatically. For methods such as LocPCA with randomness in the classification, we report the mean accuracy over 50 runs, realizing a standard deviation less than 0.1.

Our first experiment examines clustering accuracy and timing as a function of the intersection angle between two manifolds. We take two quadrants of a cylinder's lateral surface to form two 2d curved surfaces, and then intersect the surfaces at various angles α: $\frac{\pi}{2}$, $\frac{\pi}{4}$, $\frac{\pi}{8}$ and $\frac{\pi}{12}$; see Figures 1a and 1b. We first test performance in the absence of noise; see Table I for accuracy and runtimes. We then embed the data in $\mathbb{R}^{10}$ and add isotropic Gaussian noise with standard deviation $\sigma = 0.003$ in each coordinate; see Table II for performance on the noisy data. Both LAPD and PBC show robustness with respect to α, but LocPCA and SMCE produce poor results; on the noiseless data, k in LAPD is estimated correctly for all angles, while on the noisy data the estimated k is inaccurate for small α.

	LAPD (ours)		LocPCA [2]		PBC [3]		SMCE [7]	
$\alpha = \frac{\pi}{2}$	**.998**	40.0	.577	**1.1**	.981	6.7	.738	168.1
$\alpha = \frac{\pi}{4}$	**.999**	30.1	.576	**1.5**	.980	5.8	.736	150.5
$\alpha = \frac{\pi}{8}$	**.997**	30.8	.526	**4.1**	.964	8.6	.500	126.8
$\alpha = \frac{\pi}{12}$	**.992**	37.1	.539	9.0	.963	**4.3**	.500	126.5

Table I: Impact of Intersection Angle for Noiseless ($\sigma = 0$) Data in $\texttt{CS}(\alpha)$. First columns (white background) report mean clustering accuracy; second columns (gray background) report runtime (s).

In the second experiment, we conduct tests on some complex and irregular objects visualized in Figures 1c - 1h. These low-dimensional objects are once again embedded in $\mathbb{R}^{10}$ and Gaussian noise with $\sigma = 0.003$ is added to each coordinate. See Table III for cluster accuracy and runtimes. For LAPD, we estimate both d and σ using the MSVD algorithm [13], we automatically select K_1 as a function of the estimated noise level and choose $K_2 = K_1 + 10$, and we estimate k from the maximal eigengap of the landmark Laplacian (runtime includes all parameter estimates). Thus the only required input for the LAPD results in Table III is the data X and a denoising threshold which the user inputs from visual inspection of an elbow plot. For PBC, we set the angle constraint to 20 degrees; for SMCE, we set $\lambda = 10$ following [3]. For all competing methods we manually tune the locality parameter, although long runtimes for SMCE inhibited rigorous tuning. LAPD once again exhibits the highest accuracy, with PBC also performing very well; the other methods produced relatively poor results. Although LAPD and PBC were comparable in terms of performance, primary contributions of LAPD are automatic k detection and parameter selection.

	LAPD	k-LAPD	LocPCA	PBC	SMCE
$\alpha = \frac{\pi}{2}$	**0.989**	**0.989**	.563	.978	.737
$\alpha = \frac{\pi}{4}$	**0.968**	**0.968**	.579	.962	.501
$\alpha = \frac{\pi}{8}$	0.680	**0.932**	.502	.922	.500
$\alpha = \frac{\pi}{12}$	0.644	0.689	.507	**.856**	.500

Table II: Impact of Intersection Angle for Noisy Data ($\sigma = 0.003$ in $\mathbb{R}^{10}$) on $\mathtt{CS}(\alpha)$. "LAPD" automatically estimates the number of manifolds, "k-LAPD" receives the number of clusters as an input.

	LAPD (ours)		LocPCA		PBC		SMCE	
OR	**.992**	13.1	.656	3.7	.968	3.1	.990	89.3
RC	**.962**	14.5	.744	3.8	.958	3.5	.625	136.3
DS	**.995**	115.7	.979	2.2	.985	47.4	.503	5314.0
TS	**.992**	219.7	.698	7.6	.976	61.4	.847	3225.0
TP	**.974**	68.2	.505	1.7	.930	4.5	.549	338.0
SR	**.970**	194.4	.597	2.2	.927	30.6	.574	1321.0

Table III: MMC on noisy datasets in Figure 1 First column (white background) is clustering accuracy; second column (gray background) is runtime (s).

V. Conclusion

We propose and investigate a new algorithm for MMC, using angles between d-simplices as an ingredient for computing with the LAPD metric, and employ spectral clustering to automatically detect the number of manifolds. Our results demonstrate that LAPD is competitive with or superior to alternative MMC methods on nontrivial synthetic datasets. Future work will develop theoretical underpinnings for MMC with LAPD, develop more detailed complexity analysis, and explore applicability of LAPD to real-world datasets.

Acknowledgment

The authors thank Nicolás García Trillos, Daniel McKenzie, and James Murphy for useful conversations and shared code. AL thanks NSF DMS-2309570 and NSF DMS-2136198. HC and AN are partially supported by NSF DMS-1848508 and AFOSR FA9550-20-1-0338.

References

[1] Maryam Abdolali and Nicolas Gillis. "Beyond linear subspace clustering: A comparative study of nonlinear manifold clustering algorithms". en. In: *Computer Science Review* 42 (Nov. 2021), p. 100435. ISSN: 1574-0137. DOI: 10.1016/j.cosrev.2021.100435. URL: https://www.sciencedirect.com/science/article/pii/S1574013721000757 (visited on 07/12/2022).

[2] Ery Arias-Castro, Gilad Lerman, and Teng Zhang. "Spectral Clustering Based on Local PCA". In: *Journal of Machine Learning Research* 18.9 (2017), pp. 1–57. ISSN: 1533-7928. URL: http://jmlr.org/papers/v18/14-318.html (visited on 03/20/2023).

[3] Amir Babaeian, Alireza Bayestehtashk, and Mojtaba Bandarabadi. "Multiple Manifold Clustering Using Curvature Constrained Path". en. In: *PLOS ONE* 10.9 (Sept. 2015). Publisher: Public Library of Science, e0137986. ISSN: 1932-6203. DOI: 10.1371/journal.pone.0137986. URL: https://journals.plos.org/plosone/article?id=10.1371/journal.pone.0137986 (visited on 03/16/2023).

[4] R. Basri and D.W. Jacobs. "Lambertian reflectance and linear subspaces". English. In: *IEEE Transactions on Pattern Analysis and Machine Intelligence* 25.2 (2003), pp. 218–233. ISSN: 0162-8828. DOI: 10.1109/TPAMI.2003.1177153.

[5] P.S. Bradley and O.L. Mangasarian. "k-Plane Clustering". en. In: *Journal of Global Optimization* 16.1 (Jan. 2000), pp. 23–32. ISSN: 1573-2916. DOI: 10.1023/A:1008324625522. URL: https://doi.org/10.1023/A:1008324625522 (visited on 03/14/2023).

[6] J.P. Costeira and T. Kanade. "A Multibody Factorization Method for Independently Moving Objects". English. In: *International Journal of Computer Vision* 29.3 (1998), pp. 159–179. ISSN: 0920-5691. DOI: 10.1023/A:1008000628999.

[7] Ehsan Elhamifar and René Vidal. "Sparse Manifold Clustering and Embedding". In: *Advances in Neural Information Processing Systems*. Vol. 24. Curran Associates, Inc., 2011. URL: https://proceedings.neurips.cc/paper/2011/hash/fc490ca45c00b1249bbe3554a4fdf6fb-Abstract.html (visited on 03/29/2023).

[8] Ehsan Elhamifar and René Vidal. "Sparse Subspace Clustering: Algorithm, Theory, and Applications". In: *IEEE Transactions on Pattern Analysis and Machine Intelligence* 35.11 (Nov. 2013). Conference Name: IEEE Transac-

tions on Pattern Analysis and Machine Intelligence, pp. 2765–2781. ISSN: 1939-3539. DOI: 10.1109/TPAMI.2013.57.

[9] Dian Gong, Xuemei Zhao, and Gérard Medioni. "Robust multiple manifolds structure learning". In: *Proceedings of the 29th International Coference on International Conference on Machine Learning*. ICML'12. Madison, WI, USA: Omnipress, June 2012, pp. 25–32. ISBN: 978-1-4503-1285-1. (Visited on 03/29/2023).

[10] Trevor Hastie and Patrice Simard. "Metrics and Models for Handwritten Character Recognition". en. In: *Conference on Statistical Science Honouring the Bicentennial of Stefano Franscini's Birth*. Ed. by Carlo Malaguerra, Stephan Morgenthaler, and Elvezio Ronchetti. Monte Verità. Basel: Birkhäuser, 1997, pp. 203–219. ISBN: 978-3-0348-8930-8. DOI: 10.1007/978-3-0348-8930-8_16.

[11] J. Ho et al. "Clustering appearances of objects under varying illumination conditions". In: *2003 IEEE Computer Society Conference on Computer Vision and Pattern Recognition, 2003. Proceedings.* Vol. 1. ISSN: 1063-6919. June 2003, pp. I–I. DOI: 10.1109/CVPR.2003.1211332.

[12] Anna Little, Mauro Maggioni, and James M. Murphy. "Path-Based Spectral Clustering: Guarantees, Robustness to Outliers, and Fast Algorithms". In: *Journal of Machine Learning Research* 21.6 (2020). arXiv:1712.06206 [stat], pp. 1–66. URL: http://arxiv.org/abs/1712.06206 (visited on 09/16/2020).

[13] Anna V. Little, Mauro Maggioni, and Lorenzo Rosasco. "Multiscale geometric methods for data sets I: Multiscale SVD, noise and curvature". en. In: *Applied and Computational Harmonic Analysis* 43.3 (Nov. 2017), pp. 504–567. ISSN: 1063-5203. DOI: 10.1016/j.acha.2015.09.009. URL: https://www.sciencedirect.com/science/article/pii/S1063520315001414 (visited on 03/20/2023).

[14] G. Liu et al. "Robust recovery of subspace structures by low-rank representation". undefined. In: *IEEE Trans. on Pattern Analysis and Machine Intelligence* 35.1 (2012), pp. 171–184.

[15] R. Souvenir and R. Pless. "Manifold clustering". In: *Tenth IEEE International Conference on Computer Vision (ICCV'05) Volume 1*. Vol. 1. 2005, 648–653 Vol. 1. DOI: 10.1109/ICCV.2005.149.

[16] M.E. Tipping and C.M. Bishop. "Mixtures of probabilistic principal component analyzers". English. In: *Neural Computation* 11.2 (1999), pp. 443–482. ISSN: 0899-7667. DOI: 10.1162/089976699300016728.

[17] C. Tomasi and T. Kanade. "Shape and motion from image streams under orthography: a factorization method". English. In: *International Journal of Computer Vision* 9.2 (1992), pp. 137–154. ISSN: 0920-5691. DOI: 10.1007/BF00129684.

[18] Nicolas Garcia Trillos, Pengfei He, and Chenghui Li. *Large sample spectral analysis of graph-based multi-manifold clustering*. arXiv:2107.13610 [cs, math, stat]. July 2021. DOI: 10.48550/arXiv.2107.13610. URL: http://arxiv.org/abs/2107.13610 (visited on 10/25/2022).

[19] R. Vidal. "Subspace clustering". English. In: *IEEE Signal Processing Magazine* 28.2 (2011), pp. 52–68. ISSN: 1053-5888. DOI: 10.1109/MSP.2010.939739.

[20] René Vidal, Yi Ma, and S. Shankar Sastry. "Principal Component Analysis". en. In: *Generalized Principal Component Analysis*. Ed. by René Vidal, Yi Ma, and S.S. Sastry. Interdisciplinary Applied Mathematics. New York, NY: Springer, 2016, pp. 25–62. ISBN: 978-0-387-87811-9. DOI: 10.1007/978-0-387-87811-9_2. URL: https://doi.org/10.1007/978-0-387-87811-9_2 (visited on 03/14/2023).

[21] Xu Wang, Konstantinos Slavakis, and Gilad Lerman. "Multi-Manifold Modeling in Non-Euclidean spaces". In: *Proceedings of the Eighteenth International Conference on Artificial Intelligence and Statistics*. Ed. by Guy Lebanon and S. V. N. Vishwanathan. Vol. 38. Proceedings of Machine Learning Research. San Diego, California, USA: PMLR, May 9, 2015, pp. 1023–1032. URL: https://proceedings.mlr.press/v38/wang15b.html.

[22] Yong Wang et al. "Multi-manifold Clustering". In: *PRICAI 2010: Trends in Artificial Intelligence*. Ed. by Byoung-Tak Zhang and Mehmet A. Orgun. Lecture Notes in Computer Science. Berlin, Heidelberg: Springer,

2010, pp. 280–291. ISBN: 978-3-642-15246-7. DOI: 10.1007/978-3-642-15246-7_27.

[23] John Wright et al. “Robust Face Recognition via Sparse Representation”. In: *IEEE Transactions on Pattern Analysis and Machine Intelligence* 31.2 (Feb. 2009). Conference Name: IEEE Transactions on Pattern Analysis and Machine Intelligence, pp. 210–227. ISSN: 1939-3539. DOI: 10.1109/TPAMI.2008.79.

[24] Xulun Ye and Jieyu Zhao. “Multi-manifold clustering: A graph-constrained deep non-parametric method”. In: *Pattern Recognition* 93 (Sept. 1, 2019), pp. 215–227. ISSN: 0031-3203. DOI: 10.1016/j.patcog.2019.04.029. URL: https://www.sciencedirect.com/science/article/pii/S003132031930175X.

[25] Zheng Zhang et al. “A Survey of Sparse Representation: Algorithms and Applications”. In: *IEEE Access* 3 (2015). Conference Name: IEEE Access, pp. 490–530. ISSN: 2169-3536. DOI: 10.1109/ACCESS.2015.2430359.

[26] Linlin Zong et al. “Multi-view clustering via multi-manifold regularized non-negative matrix factorization”. In: *Neural Networks* 88 (Apr. 1, 2017), pp. 74–89. ISSN: 0893-6080. DOI: 10.1016/j.neunet.2017.02.003. URL: https://www.sciencedirect.com/science/article/pii/S089360801730028X.